LIQUID METAL AS HEAT TRANSFER FLUID IN DUAL-MEDIA SENSIBLE AND LATENT HEAT STORAGE

K. Niedermeier*[1], S. Sinning[1], F. Müller-Trefzer[1], L. Marocco[2], T. Wetzel[3]

[1]Institute for Thermal Energy Technology and Safety, Karlsruhe Institute of Technology (KIT), 76344 Eggenstein-Leopoldshafen, Germany
[2]Department of Energy, Politecnico di Milano, Italy
[3]Institute of Thermal Process Engineering, Karlsruhe Institute of Technology, Germany

ABSTRACT

Thermal energy storage is essential for de-coupling heat supply and demand. Especially for heat produced from fluctuating renewable energy (e.g. concentrating solar power) a heat storage system is necessary. In this study, a dual-media storage configuration using liquid metal as heat transfer fluid is presented and analysed by a numerical study. A sensible heat storage with solid filler material is compared with a partly latent heat storage (5% to 20% of the storage volume) with encapsulated phase change material. The results show that the addition of encapsulated phase change material to the dual-media storage system leads to an increase of the maximal dischargeable heat and thus, an increase of the utilization ratio. Additionally, the fluid can be extracted at constant temperature for a longer time. A comparison of different cut-off temperatures for the discharge flow shows that higher cut-off temperatures lead to a decreased utilization ratio. In general, the combined sensible-latent storage systems show less sensitivity that the sensible storage system on the chosen cut-off temperatures and are thus, more flexible regarding the connected thermal process.

1. INTRODUCTION

Liquid metals such as lead, lead-bismuth eutectic, tin or sodium have excellent heat transfer properties and are applicable in a broad operation temperature range [1]. In concentration solar power plants, for instance, in which high heat loads need to be transferred efficiently, liquid metals can be a promising alternative to the currently used molten salts in order to achieve higher thermal receiver efficiencies [2, 3].

For a reliable heat supply on demand, a thermal energy storage system is used which is a two-tank molten salt solution in most of the currently operating solar tower installations. In this work, a packed-bed heat storage solution with liquid metal as the heat transfer fluid is proposed. In this storage configuration, the main part of the thermal energy is stored in the filler material, which is either a solid material storing sensible heat or encapsulated phase change material (PCM) storing additional latent heat. The discharge process is analysed and compared for a packed-bed with ratios of 100% sensible heat storage material and 5% to 20% of the storage material being replaced by encapsulated PCM at the top of the storage tank.

2. MODEL

In order to analyse the thermal processes during charge and discharge cycles in a packed-bed storage system, a concentric dispersion model is used, in which the energy equation for the fluid and the filler material are solved with the finite volume method in an in-house code. The energy equations for the sensible heat storage case are explained in detail in previous publications [4]. The energy equation for the capsule shell is shown in Eq. 1 and for the encapsulated phase change material is presented in Eq. 2.

$$(\rho c_p)_{\mathrm{sh}} \frac{\partial T_{\mathrm{sh}}}{\partial t} = \lambda_{\mathrm{sh}} \frac{1}{z^2} \frac{\partial}{\partial z} \left(z^2 \frac{\partial T_{\mathrm{sh}}}{\partial z} \right) \tag{1}$$

*Corresponding Author: klarissa.niedermeier@kit.edu

$$(\rho c_p)_{\mathrm{PCM,eff}} \frac{\partial T_{\mathrm{PCM}}}{\partial t} = \lambda_{\mathrm{PCM,eff}} \frac{1}{y^2} \frac{\partial}{\partial y} \left(y^2 \frac{\partial T_{\mathrm{PCM}}}{\partial y} \right) \tag{2}$$

The effective volumetric heat capacity $(\rho c_p)_{\mathrm{PCM,eff}}$ and thermal conductivity $\lambda_{\mathrm{PCM,eff}}$ are calculated according to the temperature present in the encapsulated PCM (Eq. 3 and Eq. 4) as discussed in [5].

$$(\rho c_p)_{\mathrm{PCM,eff}} = \begin{cases} (\rho c_p)_{\mathrm{s}} & T_{\mathrm{PCM}} \leq T_{\mathrm{m}} - \Delta T_{\mathrm{m}} \\ \dfrac{\bar{\rho} \Delta H_{\mathrm{m}}}{2 \Delta T_{\mathrm{m}}} + (1 - z_{\mathrm{l}}) \left(\rho c_p\right)_{\mathrm{s}} + z_{\mathrm{l}} \left(\rho c_p\right)_{\mathrm{l}} & T_{\mathrm{m}} - \Delta T_{\mathrm{m}} < T_{\mathrm{PCM}} < T_{\mathrm{m}} + \Delta T_{\mathrm{m}} \\ (\rho c_p)_{\mathrm{l}} & T_{\mathrm{PCM}} \geq T_{\mathrm{m}} + \Delta T_{\mathrm{m}} \end{cases} \tag{3}$$

$$\lambda_{\mathrm{PCM,eff}} = \begin{cases} \lambda_{\mathrm{s}} & T_{\mathrm{PCM}} \leq T_{\mathrm{m}} - \Delta T_{\mathrm{m}} \\ (1 - z_{\mathrm{l}}) \lambda_{\mathrm{s}} + z_{\mathrm{l}} \lambda_{\mathrm{l}} & T_{\mathrm{m}} - \Delta T_{\mathrm{m}} < T_{\mathrm{PCM}} < T_{\mathrm{m}} + \Delta T_{\mathrm{m}} \\ \lambda_{\mathrm{l}} & T_{\mathrm{PCM}} \geq T_{\mathrm{m}} + \Delta T_{\mathrm{m}} \end{cases} \tag{4}$$

In the temperature region below the melting temperature T_{m} (incl. a melting temperature range of $2\Delta T_{\mathrm{m}}$), the properties of the solid (s) PCM are taken, above the melting temperature the properties of the liquid (l) PCM are used. At the melting temperature (incl. a melting temperature range of $2\Delta T_{\mathrm{m}}$) the properties are calculated according to the liquid phase fraction (Eq. 5).

$$z_{\mathrm{l}} = \frac{T_{\mathrm{PCM}} - T_{\mathrm{m}} + \Delta T_{\mathrm{m}}}{2 \Delta T_{\mathrm{m}}} \tag{5}$$

A second-order Crank-Nicolson scheme is used for the time discretization, a central difference scheme for the diffusive and an upwind scheme for the advective terms.

The boundary condition for the fluid is a constant temperature (Dirichlet) at the inlet of the tank and zero heat flux (Neumann) at the outlet. The solid filler spheres, in the sensible heat storage case, are coupled with the fluid with a convection boundary condition at the outer surface and have a symmetry condition at the centre. In the latent heat storage case, the capsule shell is coupled to the fluid analogously with a convection boundary condition at the outer surface and coupled to the PCM with a Neumann boundary condition. The PCM has a symmetry boundary condition in the centre.

3. REFERENCE CASE

The simulation is performed starting from a fully charged heat storage with a homogeneous temperature (700 °C) in the fluid, PCM and capsule shell. The storage is then completely discharged for a sensible heat configuration and combined sensible-latent configurations (5% to 20% of encapsulated PCM). The liquid metal is lead-bismuth eutectic and the storage dimensions (tank height H = 2 m and tank diameter D = 0.6 m) and bed porosity (ε = 0.37) are similar to a currently planned experimental demonstration of a dual-media sensible heat storage at the Karlsruhe Liquid Metal Laboratory at KIT. Table 1 presents the thermo-physical properties and the melting temperatures of lead-bismuth eutectic.

Table 1: Thermo-physical properties and melting temperature of the liquid metal lead-bismuth eutectic at 600 °C [6].

c_p / Jkg^{-3}K^{-1}	ρ / kgm^{-3}	ρc_p / kJm^{-3}K^{-1}	λ / Wm^{-1}K^{-1}	T_{m} / °C
141	9940	1398	16	125

As filler material in the sensible thermal energy storage system, zirconium silicate is selected for the simulation, as this has proven to be compatible with the liquid metal lead-bismuth-eutectic in previous experiments. For the simulation of the latent thermal energy storage part, AlSi is chosen as the phase change material (PCM) and alumina as the capsule shell material. The outer diameter of the capsule

shell is defined as the same size as the solid filler material (d = 20 mm). Other PCM candidates for the temperature range above 500°C are salts, metals and metal alloys. An overview is given in Ref. [7].

Table 2 shows the thermo-physical properties of the filler material: the volumetric heat capacity ρc_p, the thermal conductivity λ and the melting enthalpy ΔH_m of the PCM. For the PCM, the properties of both the solid (s) and the liquid (l) are presented.

Table 2: Thermo-physical properties of the filler material.

	Solid filler: Zirconium silicate [8]	*Latent filler - PCM:* Al-19.7Si [9,10]	*Latent filler - capsule shell:* Al_2O_3 [11]
$(\rho c_p)_\mathrm{s}$ / kJm^{-3}K^{-1}	4659	3708	3423
$(\rho c_p)_\mathrm{l}$ / kJm^{-3}K^{-1}	-	4260	-
λ_s / Wm^{-1}K^{-1}	7.5	220	35
λ_l / Wm^{-1}K^{-1}	-	70	-
ΔH_m / kJkg^{-1}	-	478	-

The storage parameters for the simulations performed in this work are summarized in Fig. 2.

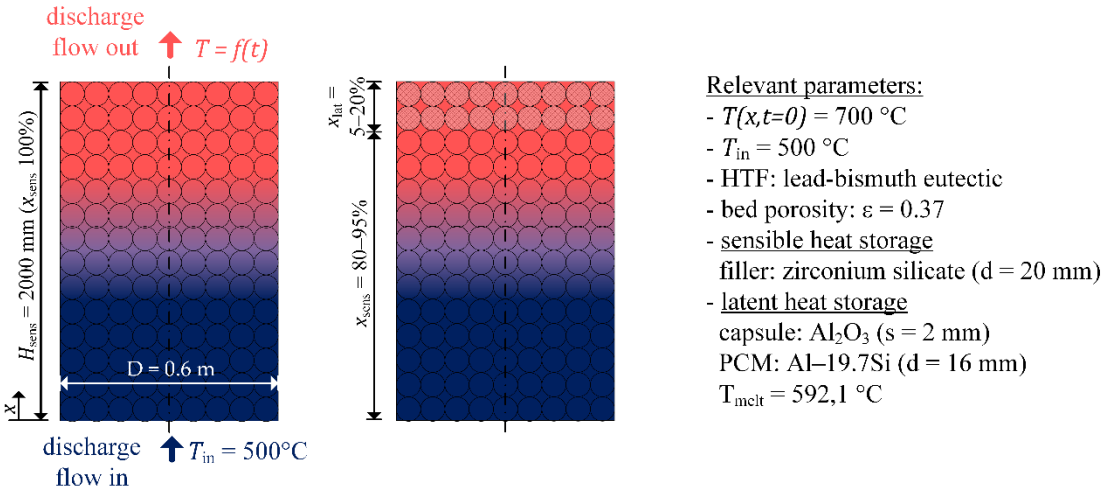

Figure 1: Schematic of dual-media thermal energy storage systems; left: sensible heat storage with solid filler material; centre: part of the filler material is replaced by PCM at the hot end; right: relevant storage parameters for the simulation.

4. RESULTS

Figure 3 shows the temperature of the liquid metal leaving the top of the storage tank. It can be observed that already a small amount of encapsulated PCM at the top of the tank leads to a stabilization of the outlet temperature at the melting temperature of the PCM for some minutes. The more PCM is included in the storage, the longer the fluid can be extracted at the melting temperature. Depending on the following process, a PCM with a suitable melting temperature needs to be selected. In this study, a cut-off temperature of 580 °C is defined in order to assess the amount of thermal energy that can be extracted until the fluid outlet temperature reached this value.

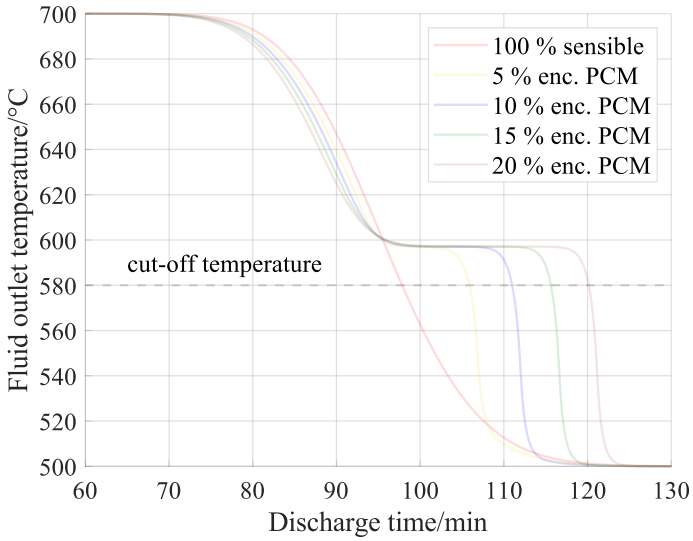

Figure 2: Fluid outlet temperature during discharge for a sensible heat storage configuration and combined sensible-latent heat storage configurations (5% to 20% encapsulated PCM).

In Table 3, the dischargeable heat for a complete discharge cycle and for a cut-off temperature at 580 °C are presented as well as their ratio - the utilization ratio (UR) - and the discharge time at constant melting temperature.

Table 3: Dischargeable heat (Q), utilization ratio (UR) and the time, in which the heat can be extracted at melting temperature (t_{stable}).

Filler material cases	$Q_{dis,max}$/ kWh	$Q_{dis,cut-off}$/ kWh	UR/ %	t_{stable}/ min
100% sensible	108.5	105.4	97.1	0
5% enc. PCM, 95% sensible	110.6	109.6	99.1	5.3
10% enc. PCM, 90% sensible	112.8	112.1	99.4	9.8
15% enc. PCM, 85% sensible	114.9	114.3	99.5	13.9
20% enc. PCM, 80% sensible	117.1	116.5	99.5	18.0

It can be concluded that adding encapsulated PCM leads to an increase of the storage density, an addition of 5% PCM leads to an increase of 1.9% in the maximal dischargeable heat and 4.0% in the dischargeable heat for a cut-off temperature at 580 °C. That leads to a raise of 2.0% in the utilization ratio. When adding 20% of PCM, the utilization ratio is not significantly increased, however, the time, in which the fluid flow can be extracted at constant temperature can be improved by a factor of three.

Figure 4 shows the influence of the cut-off temperature on the utilization ratio. With increasing cut-off temperature the utilization ratio decreases. For the sensible storage configuration it is 2%, if the cut-off temperature is changed from 520 °C to 580 °C. For the latent storage configuration the trend is similar, yet less pronounced, the difference in the utilization ratios is only up to 0.5 %. This leads to the conclusion that a combined sensible-latent heat storage system is less sensitive on the cut-off temperature that is needed for the connected thermal process. However, this depends on the melting temperature of the PCM.

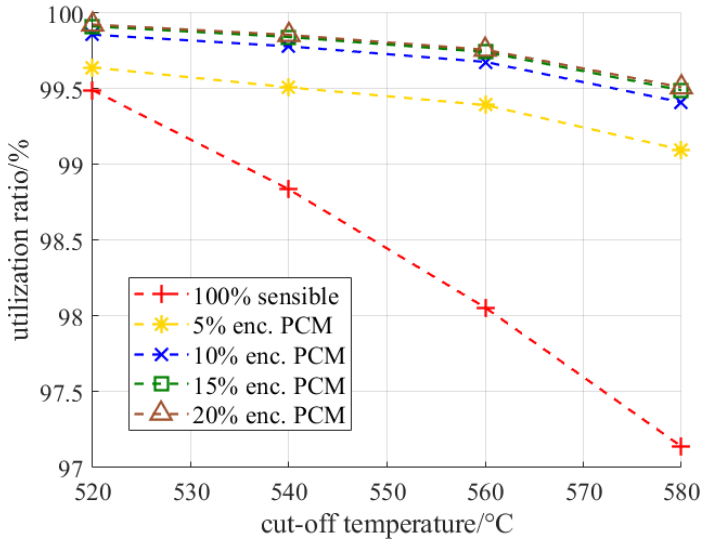

Figure 4: Utilization ratio depending on the cut-off temperature for a sensible heat storage configuration and combined sensible-latent heat storage configurations (5% to 20% encapsulated PCM).

5. CONCLUSIONS

Simulations of dual-media storage configurations with liquid metal as heat transfer fluid are performed with sensible heat storage material and additional encapsulated PCM at the top of the storage tank. The energy equations are solved for the fluid, the PCM and the capsule shell. The results show that already for small amounts of encapsulated PCM, the storage capacity can be increased by 2.0% and the outlet temperature can be stabilized at the melting temperature for several minutes.

REFERENCES

[1] J. Pacio & Th. Wetzel, Assessment of liquid metal technology status and research paths for their use as efficient heat transfer fluids in solar central receiver systems. *Solar Energy*, **93** (2013) 11–12.

[2] A. Fritsch, C. Frantz & R. Uhlig, Techno-economic analysis of solar thermal power plants using liquid sodium as heat transfer fluid. *Solar Energy*, **177** (2019) 155–162.

[3] J. Coventry, C. Andraka, J. Pye, M. Blanco & J. Fisher, A review of sodium receiver technologies for central receiver solar power plants. *Solar Energy*, **122** (2015) 749–762.

[4] K. Niedermeier, L. Marocco, J. Flesch, G. Mohan, J. Coventry & T. Wetzel, Performance of molten sodium vs. molten salts in a packed bed thermal energy storage. *Applied Thermal Engineering*, **141** (2018) 368–377.

[5] S. Liu, Y. Li, Y. Zhang, Mathematical solutions and numerical models employed for the investigations of PCMs' phase transformations. *Renewable and Sustainable Energy Reviews*, **33** (2014) 659–674.

[6] OECD-NEA, *Handbook on Lead-bismuth Eutectic Alloy and Lead Properties, Materials Compatibility, Thermal-hydraulics and Technologies*, (2007).

[7] B. Cárdenas & N. León, High temperature latent heat thermal energy storage: Phase change materials, design considerations and performance enhancement techniques. *Renewable and Sustainable Energy Reviews*, **27** (2013), 724–737.

[8] E. Kleinert, private communication, 2020. Material data Rimax® Saint-Gobain.

[9] G .Wei, P. Huang, C. Xu, D. Liu, X. Ju, X. Du, L. Xing, Y. Yang, Thermophysical property measurements and thermal energy storage capacity analysis of aluminum alloys, *Solar Energy*, **137** (2016), 66–72.

[10] D. R. Poirier, Density, Viscosity, and Diffusion Coefficients in Hypoeutectic Al-Si Liquid Alloys: An Assessment of Available Data, *Metallurgical and Materials Transactions B*, **45** (2014), 1345–1354.

[11] Accuratus, 99.5 % Alumina Material Properties. [Online]. https://accuratus.com/alumox html (Access: 14th January 2022).